Follow us @BoneJointRes

Freely available online OPEN ACCESS

BJR

BIOMECHANICS

Importance of posterior tibial slope in joint kinematics with an anterior cruciate ligament-deficient knee

L. Shu,
N. Abe,
S. Li,
N. Sugita

From The University of Tokyo, Tokyo, Japan

Aims
To fully quantify the effect of posterior tibial slope (PTS) angles on joint kinematics and contact mechanics of intact and anterior cruciate ligament-deficient (ACLD) knees during the gait cycle.

Methods
In this controlled laboratory study, we developed an original multiscale subject-specific finite element musculoskeletal framework model and integrated it with the tibiofemoral and patellofemoral joints with high-fidelity joint motion representations, to investigate the effects of 2.5° increases in PTS angles on joint dynamics and contact mechanics during the gait cycle.

Results
The ACL tensile force in the intact knee was significantly affected with increasing PTS angle. Considerable differences were observed in kinematics and initial posterior femoral translation between the intact and ACLD joints as the PTS angles increased by more than 2.5° (beyond 11.4°). Additionally, a higher contact stress was detected in the peripheral posterior horn areas of the menisci with increasing PTS angle during the gait cycle. The maximum tensile force on the horn of the medial meniscus increased from 73.9 N to 172.4 N in the ACLD joint with increasing PTS angles.

Conclusion
Knee joint instability and larger loading on the medial meniscus were found on the ACLD knee even at a 2.5° increase in PTS angle (larger than 11.4°). Our biomechanical findings support recent clinical evidence of a high risk of failure of ACL reconstruction with steeper PTS and the necessity of ACL reconstruction, which would prevent meniscus tear and thus the development or progression of osteoarthritis.

Cite this article: *Bone Joint Res* 2022;11(10):739–750.

Keywords: Anterior cruciate ligament deficiency, Osteoarthritis knee, Posterior tibial slope, Meniscus tear

Article focus
- There is a trend of greater posterior femoral translation and external femoral rotation as posterior tibial slope (PTS) increases in both anterior cruciate ligament (ACL)-intact and deficient knees.
- As for the menisci and cartilage contact pressure, there was a greater increase in contact pressure in the anterior cruciate ligament-deficient (ACLD) knee than in the intact knee as the PTS increased.

Key messages
- The joint kinematics, contact pressure, and meniscus horn force exhibited significant differences between intact and ACLD knees as the PTS angle increased beyond 11.4°.

Strengths and limitations
- Newly developed computational models are gaining increased interest due to their high efficiency, low cost, and comprehensive insight into the biomechanics of joints.
- Our novel finite element-musculoskeletal (FE-MS) framework model was

Correspondence should be sent to Nobuhiro Abe; email: nobuabe@med.kawasaki-m.ac.jp

doi: 10.1302/2046-3758.1110.BJR-2022-0039.R1

Bone Joint Res 2022;11(10):739–750.

constructed based only on a single subject, and a population-based dynamic performance of the knee joint should be further analyzed.

Introduction

Anterior cruciate ligament (ACL) injury is associated with common sports involving pivoting or twisting movements and is a hidden risk of developing knee osteoarthritis (OA). Over 50% of patients develop OA ten years after anterior cruciate ligament deficiency (ACLD).[1,2] One of the main risk factors for the development of post-traumatic knee OA is abnormal knee kinematics and mechanics during daily activities.[3-6] Additionally, the meniscus sustains repetitive damage over several years due to ACLD, which may accelerate the development of OA.[7] Thus, quantifying the dynamic environment of the ACLD knee is crucial for developing a successful treatment plan, considering factors such as the timing of surgery, meniscus injury, and prevention of cartilage degeneration.

It is technically difficult to comprehensively investigate the dynamic conditions of the knee joint, such as joint contact and soft-tissue forces, using experiments.[8] Thus, previous studies have focused on analyzing the kinematic differences between intact knees and knees with ACLD through in vivo or in vitro approaches. Shabani et al[5] presented an excessive internal tibial rotation with no significant differences in anteroposterior (AP) femoral translation between an intact and an ACLD knee using 3D in vivo motion analysis during the gait cycle. However, Chen et al[9] found that the tibia tended to shift more anteriorly in knees with ACLD than in intact knees. This discrepancy may be due to differences in anatomical factors, such as body weight, generalized joint laxity, foot pronation, and posterior tibial slope (PTS). The effect of PTS on ACLD knees has attracted considerable attention.[10-15] Increased PTS results in a greater anterior shift of the tibia during quadriceps contraction, which may increase the risk of meniscus damage and knee OA.[16] Thus, it is necessary to clarify the effect of PTS on the joint kinetics of intact and ACLD knees.

In vitro experiments provide a controlled and repeatable tool for evaluating joint mechanics;[12,17] however, the number and type of experimental tests that can be performed are limited by the need for physical parts, cadaveric specimens, and time to perform each evaluation.[18] Thus, computational models have generated great interest due to their high efficiency, low cost, and comprehensive insight into the biomechanics of soft-tissues and joints. Guess and Razu[19] investigated the loading difference between intact and ACLD knees using a multibody computational model under a non-weightbearing condition. Recently, Ali et al[8,20] developed a comprehensive knee model including the tibiofemoral (TF) and patellofemoral (PF) joints with detailed ligamentous constraints based on the Kansas Knee Simulator. They used the model to investigate differences in kinematics and ligament loading between intact knees and knees with ACLD knees during the gait cycle, and found a notable increase in anterior tibial translation and internal rotation in the ACLD knee. However, the stress pattern of the ACLD knee, which is one of the main evaluation indexes for meniscus damage and the development of OA, was not investigated. Furthermore, the effects of muscle force on joint kinematics and mechanics were not considered or were inconclusive. The force of the quadriceps is constantly overestimated during simulation compared to electromyographical data and musculoskeletal predictions.[18,21,22] The integrated finite element-musculoskeletal (FE-MS) framework evaluates knee joint loading and muscle activation, and has certified consistency between predicted and experimental results.[23,24]

Herein, we aimed to develop a high-fidelity intact knee joint model with the TF and PF joints that could be dynamically integrated into a subject-specific FE-MS framework, to understand the effects of ACLD on joint dynamics with different PTS angles during the gait cycle.

Methods

FE-MS model. We used a subject-specific FE-MS lower limb model previously validated by Shu et al,[23] which was developed to analyze the mechanics of the prosthetic knee after total knee arthroplasty. Further, our model was extended to a concurrent intact finite element (FE) knee model to estimate joint kinematics and contact mechanics of the knee, which was validated by motion capture experiments that assessed joint kinematics and grand reaction forces during the gait cycle,[24] as shown in Figure 1.

This new generic FE-MS model was developed based on anatomical data from Biomechanical Data Resources,[25] and modelled using the commercial software Abaqus CAE v2021 (Dassault Systèmes, France). Static optimization was used to determine the optimal muscle force by minimizing the metabolic energy of all the muscles that contribute to the balance of the moment around each joint.[23] Secondary knee joint kinematics were controlled by muscle force, ligament constraints, joint contact force, and the anatomical geometry of the knee. Thus, the PF joint in the current model was additionally modelled with six degrees of freedom, with ligament and contact constraints in the FE-MS model, rather than being controlled by the flexion-extension angle of the TF joint.

Knee model. We developed the intact knee model based on data from the Open Knee(s) project site.[26] The FE knee model includes bony structures (tibia, patella, and femur), major TF and PF joint ligaments (ACL, medial collateral ligament, lateral collateral ligament, posterior cruciate ligament, medial PF ligament, and lateral PF ligament), meniscus, and cartilage. A fine-meshed knee model was created using a proprietary

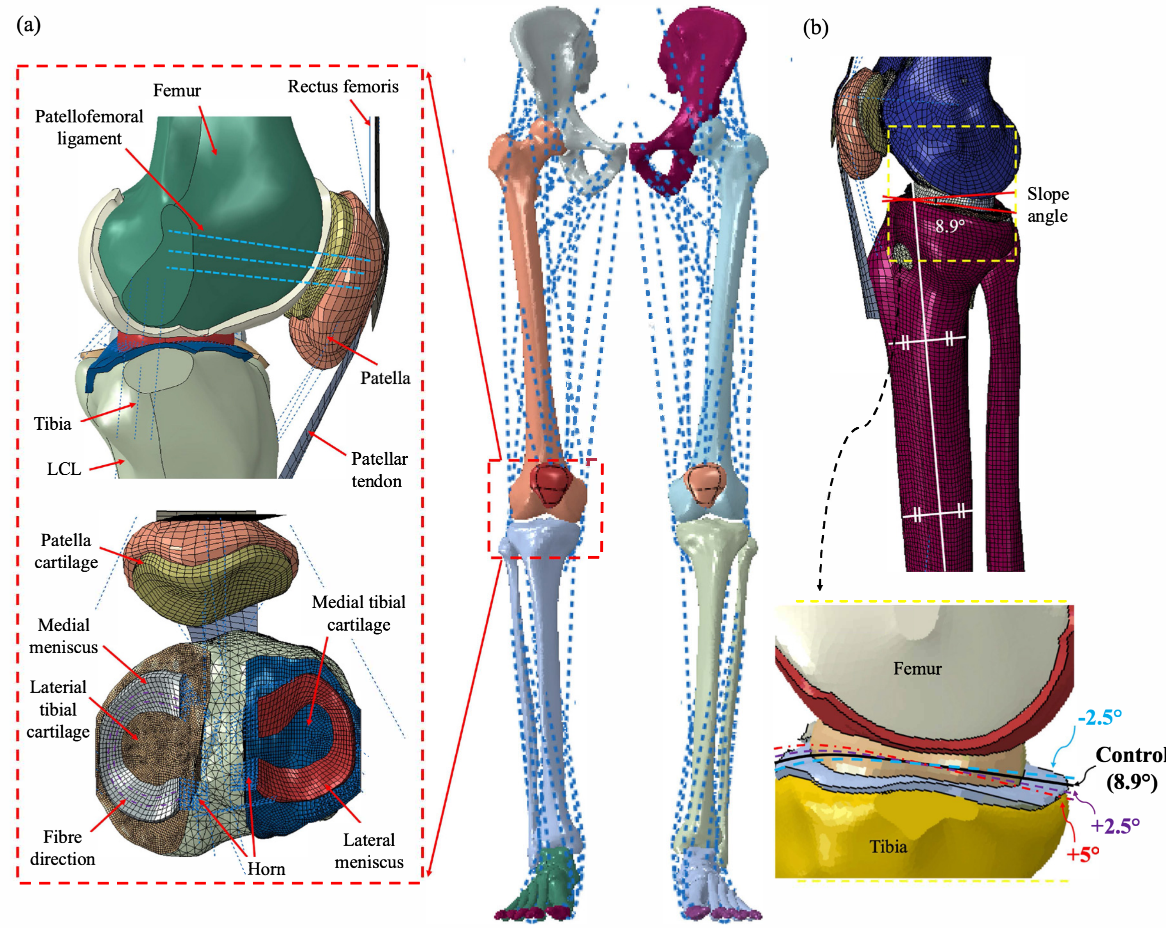

Fig. 1

a) Finite element musculoskeletal model with an intact knee. b) The original posterior tibial slope (PTS) angle was 8.9° and was defined as the standard angle. LCL, lateral collateral ligament.

FE pre-processor (Hypermesh; Altair Engineering, USA). Bony structures were modelled as a rigid body due to their high stiffness compared to soft-tissues and then pressed using the C3D4 tetrahedron element. The cartilage structures and menisci were modelled as C3D8R hexahedral elements with lengths of 0.8 mm and 1.2 mm, respectively, based on the mesh convergence analysis. The patellar tendon and rectus femoris were modelled as 2D fibre-reinforced structures, which included a membrane (M3D4R) and spring element (CONN3D2), to enhance the ligament-to-bone or component interactions in the simulation. To reduce computational overflow, the ligaments were simplified as multisegmented 1D axial connectors with no compressive stiffness instead of 3D models. The force exerted by these ligaments followed a non-linear piecewise force-displacement relationship. The stiffness-force relationship of the ligaments was modelled to produce non-linear elastic characteristics with respect to the slack region, which has been extensively used in previous studies (Table I).[20,23,24,27]

Material property and boundary condition. We modelled the articular cartilage and menisci as a nonlinear neo-Hookean hyperelastic isotropic material,[28] and a Holzapfel-Gasser-Ogden hyperelastic anisotropic material,[29] respectively. The detailed constants of cartilage and menisci (Table II) were established based on experimental compressive tests from Naghibi Beidokhti et al[30] and Tissakht and Ahmed,[31] respectively. The fibre direction of the meniscus was oriented circumferentially, as shown in Figure 1. The horns of the meniscus were represented as bundles of non-compressible springs. The horn attachments were modelled with 40 springs with an elasticity of 40 N/mm, while the anterior and posterior meniscofemoral ligaments were set as four springs with an elasticity of 12.25 N/mm.[32,33]

Table I. Material constants for ligaments in finite element knee model.[24]

Ligaments	aLCL	mLCL	pLCL	aMCL	mMCL	pMCL	aPCL	pPCL	aACL	pACL
Prestrain: (ε)	-0.01	0.03	0.02	0.04	0.08	-0.03	-0.29	-0.14	-0.05	0.07
Stiffness-force: (N)	1,937	1,883	1,985	2,112	2,644	2,115	8,214	6,146	5,576	4,901

a, anterior; ACL, anterior cruciate ligament; LCL, lateral cruciate ligament; m, middle; MCL, medial cruciate ligament; p, posterior; PCL, posterior cruciate ligament.

Table II. Material coefficients of the meniscus and cartilage.[30,31]

Part	C_{10}, MPa	D, MPa^{-1}	k_1	k_2	k
Cartilage	0.86	0.048	N/A	N/A	N/A
Medial meniscus	1	0.005	5.04	0.889	0
Lateral meniscus	1	0.005	8.48	1.559	0

N/A, not available.

General contact with a frictionless contact property was assigned to all contact pairs as in previous computational models.[12,20] We acquired the ground reaction force and marker trajectory during the gait cycle using an optical motion capture system on a healthy male participant, with no previous knee surgery and no meniscal or cruciate ligament injury (aged 28 years; height, 183 cm; body weight, 65 kg). We conducted these datasets to evaluate the loading distribution in the knee joint during gait.[24]

Design of experiments. We investigated the effects of PTS on joint dynamics in intact knees and in knees with ACLD. The original PTS angle, characterized as the angle between the line perpendicular to the middle diaphysis and the tangent to the medial tibial plateau of the knee,[34] was 8.9° and was defined as the standard angle. We modified the PTS angle in the knee model by tilting the proximal tibial metaphysis like an osteotomy to investigate the effect of different PTS angles on joint dynamics in the knee, as shown in Figure 2. Furthermore, the coordinates of muscle, ligament, and tendon attachments around the tibial plateau were rotated accordingly. It is important to determine the standard PTS angle, which was established according to realistic anatomical measurements based on those of human subjects. To investigate the effects of a steep or flat PTS on ligament loading and joint dynamics in intact knees and knees with ACLD, we incrementally increased the angle of the PTS by 2.5°. Therefore, in this study, we investigated four PTS angles ranging from 6.4° to 13.9° in increments of 2.5° (2.5° minus (6.4°), standard (8.9°), 2.5° plus (11.4°), and 5° plus (13.9°)) (Figure 2). The primary outcomes focused on the effect of PTS on the loading of the ACL and meniscus in the gait cycle. Furthermore, the corresponding kinematics and contact mechanics of the TF joint were assessed. In addition, we simulated the effect of ACLD on joint dynamics. We have summarized the simulated conditions in detail in Table III.

Results

Effect of the PTS angle on ACL tensile force. The tensile force of the ACL increased with an increasing PTS angle, as shown in Figure 3. The posterolateral (PL) bundle of the ACL carried most of the tensile force during the gait cycle at a smaller PTS angle. However, we found a higher tensile force on the anteromedial (AM) bundle of the ACL with a larger PTS angle (+5°). The tensile forces of the ACL increased during the stance phase of the gait cycle. In the control group (standard), two loading peaks on the PL bundle were found at the left toe-off (15%) and right toe-off (63%) points of the gait cycle. However, we found a different force pattern with larger PTS angles (+2.5° and +5°), and the loading peak was found at 64% of the gait cycle. The tensile force of the ACL increased from 22.3 N to 298.4 N (133.8%) when the PTS angle changed from 6.4° to 13.9°.

Kinematics. The femur tends to translate posteriorly and rotate externally with an increase in the PTS angle in both intact and ACLD knees, as shown in Figure 4. We found a small kinematical difference (posterior femoral translation less than 0.5 mm, external rotation less than 1.2°) between intact and ACLD knees in the -2.5° PTS angle. The largest difference in posterior femoral translation and external rotation was 10.8 mm and 14.5°, respectively, which were found at +5° PTS angle. Furthermore, we found a smaller kinematical difference with +5° PTS angle compared to that with +2.5° PTS angle, which may explain the different tensions in the meniscus in different PTS conditions.

Contact pressure (compression strain). The compression of the contact contour on the intact and ACLD knees at the maximum axial loading (1,842.5 N) is shown in Figure 5. At an angle of -2.5° PTS, we did not observe any significant differences in the contact pattern between the two knees. The highest compression strain was found in the medial cartilage (7.8 MPa). As the PTS angle increased, we observed a greater increase in contact pressure on the menisci and cartilage in the ACLD knee than in the intact knee. The maximum compression strains in the ACLD knee at a +5° angle of PTS were found in the medial cartilage (15.3 MPa/135%) and in the meniscus (10.2 MPa/120%), which were much higher than those of the intact knee (11.3 MPa and 8.5 MPa, respectively). The pattern of stress concentration was along the radial direction at the posterior root of the medial meniscus and extended broadly at the posterior horn of the lateral meniscus.

Tensile force of the meniscal horn root. The predicted tensile force on the posterior horn and the root of the lateral meniscus (LP) increased greatly with the angle of the PTS, while no significant differences were found on the anterior horn of the lateral meniscus (LA), as

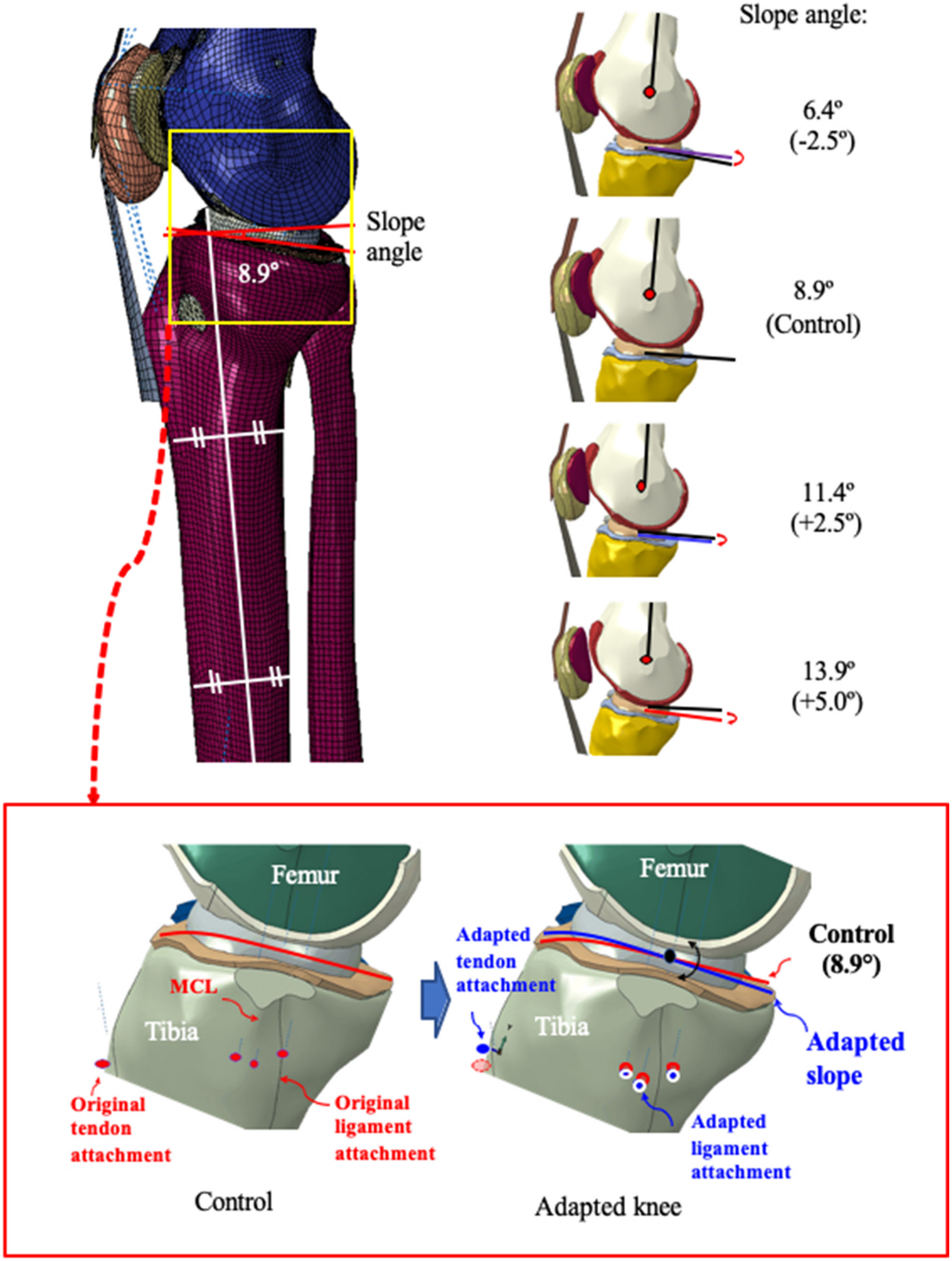

Fig. 2

Adapted knee model with different posterior tibial slope (PTS) angles in the tibial plateau. The muscle, ligament, and tendon attachments around the tibial plateau were correlately applied with modified PTS angles. MCL, medial cruciate ligament.

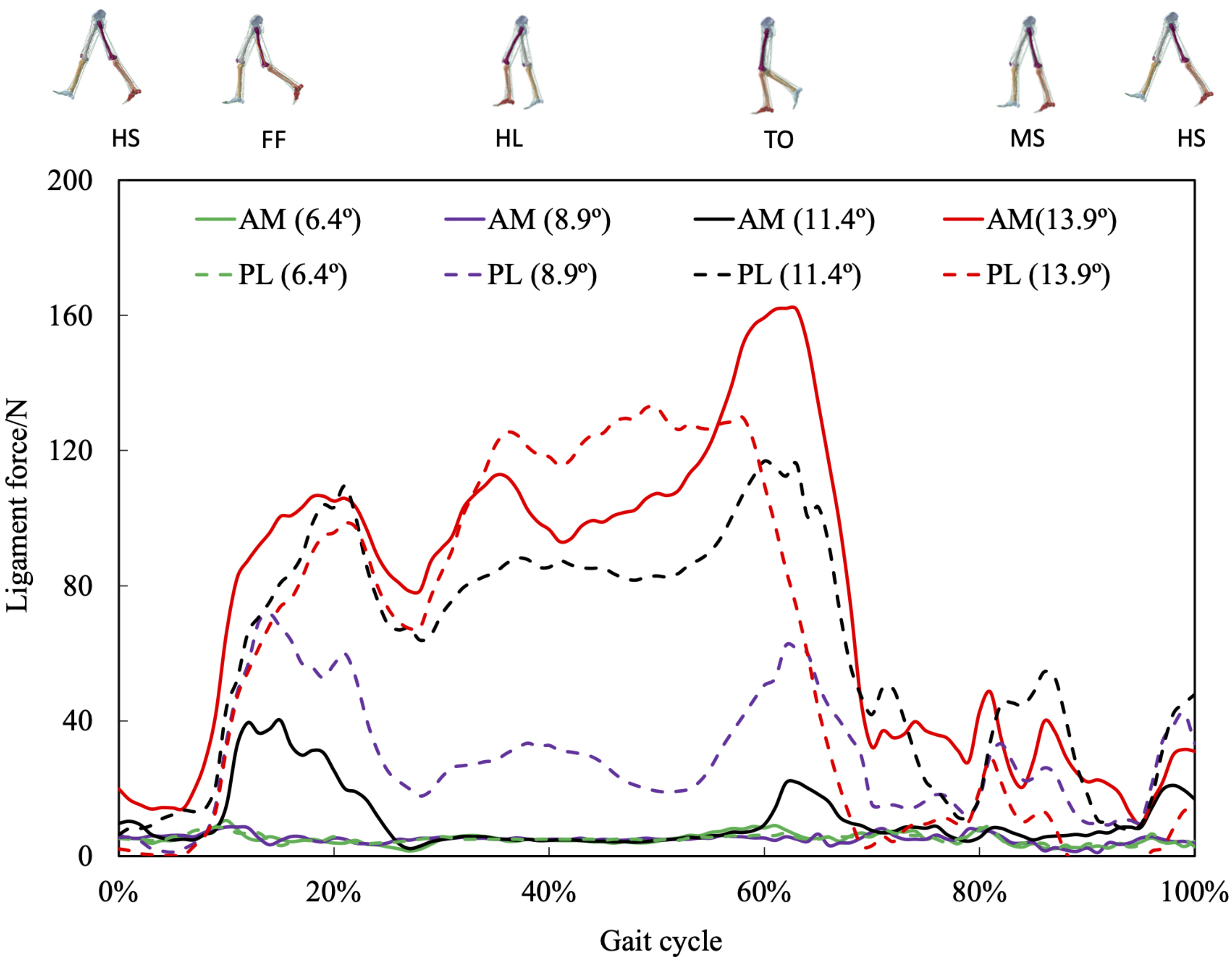

Fig. 3

Effect of the posterior tibial slope (PTS) angle on the predicted tensile force of the anterior cruciate ligament (ACL) in an intact knee joint. AM, anteromedial bundle; FF, foot flat; HL, heel lift; HS, heel strike; MS, midstance; PL, posterolateral bundle; TO, toe-off.

shown in Figure 6a. Furthermore, the ACLD knee had a much larger tensile force on the LA than the intact knee. In the medial meniscus, the tensile force of the anterior and posterior horn roots (MA and MP, respectively) increased with the PTS angle. The difference in the tensile force of the meniscal horn roots between the intact and ACLD knees increased with the PTS angle, as shown in Figure 6b. The maximum predicted tensile forces in the MP and LP were 172.3 N and 135.5 N, respectively, in the ACLD knee. We summarized the changes in the maximum tensile force on the roots of the meniscus horn with ACLD in Figure 7. The variation in the maximum tensile force changed greatly with the PTS angle.

Discussion

Herein, we coupled an in vivo experimental evaluation of the FE-MS model with a model consisting of intact knees and knees with ACLD to better understand the effects of ACLD on dynamic performance at different PTS angles. The numerical results suggested that the PTS angle plays an important role in the dynamic performance of intact and ACLD knees. Therefore, we suggest that this should be carefully considered in clinical treatment and surgical planning. In ACLD, a large PTS angle increased the risk of chronic instability, and thus the contact points of the cartilage shifted to the extreme posterior boundary of the tibial cartilage and the posterior horn roots of both the medial and lateral menisci. This resulted in heightened contact pressures

Table III. Simulation conditions.

PTS angle	Knee condition
-2.5° (6.4°)	Intact, ACLD
Standard (8.9° control)	Intact (control), ACLD
+2.5° (11.4°)	Intact, ACLD
+5° (13.9°)	Intact, ACLD

ACLD, anterior cruciate ligament deficiency; PTS, posterior tibial slope.

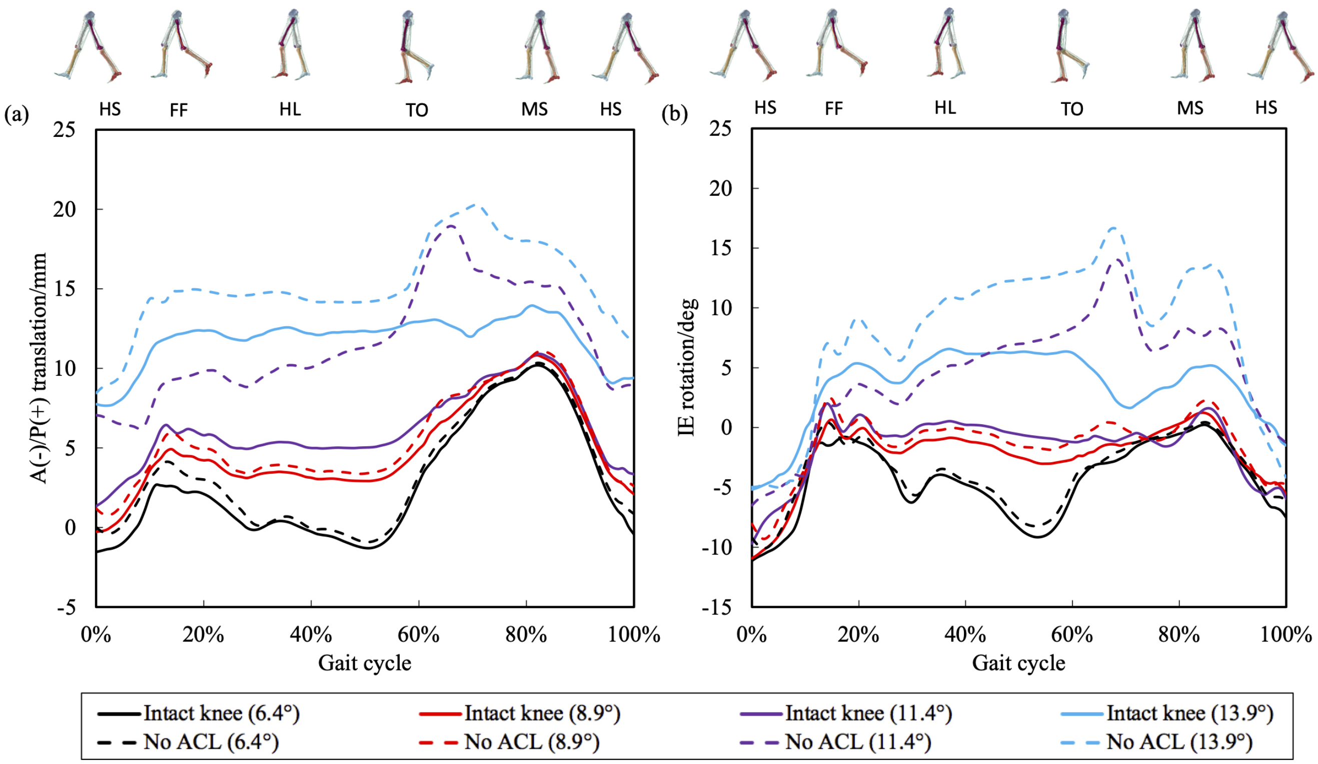

Fig. 4

Predicted kinematics of the knee joint. a) Effect of the posterior tibial slope (PTS) angle on the anteroposterior (AP) translation in an intact knee and in an anterior cruciate ligament-deficient (ACLD) knee. b) Effect of the PTS angle on the internal or external (I-E) rotation in an intact knee and an ACLD knee. FF, foot flat; HL, heel lift; HS, heel strike; MS, midstance; TO, toe-off.

that may lead to secondary meniscus and cartilage damage following ACLD.

In the intact knee, a larger PTS angle significantly increased the tensile force of the ACL, which may lead to an increased risk of ACL injury (Figure 3). Todd et al[35] investigated the relationship between the PTS angle and ACLD by digitally measuring the PTS angle in 140 non-contact ACLD knees and in 179 intact knees. Their results regarding changes in the ACL force in response to changes in the PTS angle demonstrated that knees with a non-contact ACL injury had a larger mean PTS angle (9.8° (standard deviation (SD) 2.6°) than intact knees (8.2° (SD 2.4°)).[35] Furthermore, a slope-reducing anterior wedge osteotomy could reportedly improve long-term outcomes of patients and may be beneficial in protecting the ACL graft in cases of second revision surgery.[10,36] In agreement with previous studies, our results also demonstrated that the AM bundle controls knee stability to a greater extent than the PL bundle at a larger PTS angle.[37-39] Our study results suggested that the AM bundle encountered a significant force as the PTS angle increased beyond 11.4°. Samuelsen et al[40] also highlighted that the increase in the angle of PTS would lead to a linear increase in the ACL graft force; this effect is magnified in the concomitant medial meniscus posterior root tear (MMPRT). A slope-changing osteotomy should be considered in the setting of an ACL reconstruction surgery if the PTS angle is greater than 12°. Additionally, the boundary condition in most of the previous in vitro experimental studies was controlled with a constant load in the static condition.[10,35,41] For instance, compressive loading in the study by Bernhardson et al[10] was 200 N, which is much less than the loading in the knee joint. The maximum joint loading during the gait cycle and squatting is approximately 2.67 and 3.1 times greater than that of body weight, respectively.[42] The high-fidelity computational model provides easy access and facilitates a low-cost and comprehensive approach to preclinical analysis and planning.

The change in kinematics between intact and ACLD knees can have a great impact on knee stability and result in cartilage damage and OA.[43] Here, we observed a similar kinematic pattern in the control group (PTS angle: 8.9°) between the predicted results and the previous state-of-the-art 3D fluoroscopic measurements in vivo taken during the gait cycle.[19] Overall, ACLD resulted in greater posterior femoral translation and external rotation. We also found that the change in kinematics due to ACLD was highly dependent on the PTS angle. This explains the contradictory conclusions in clinical studies. Shabani et al[5] found slightly more posterior femoral translation during most of the gait cycle, while no significant differences were reported in knee joint translation compared to intact knee joint using 3D in vivo motion analysis during the gait cycle.

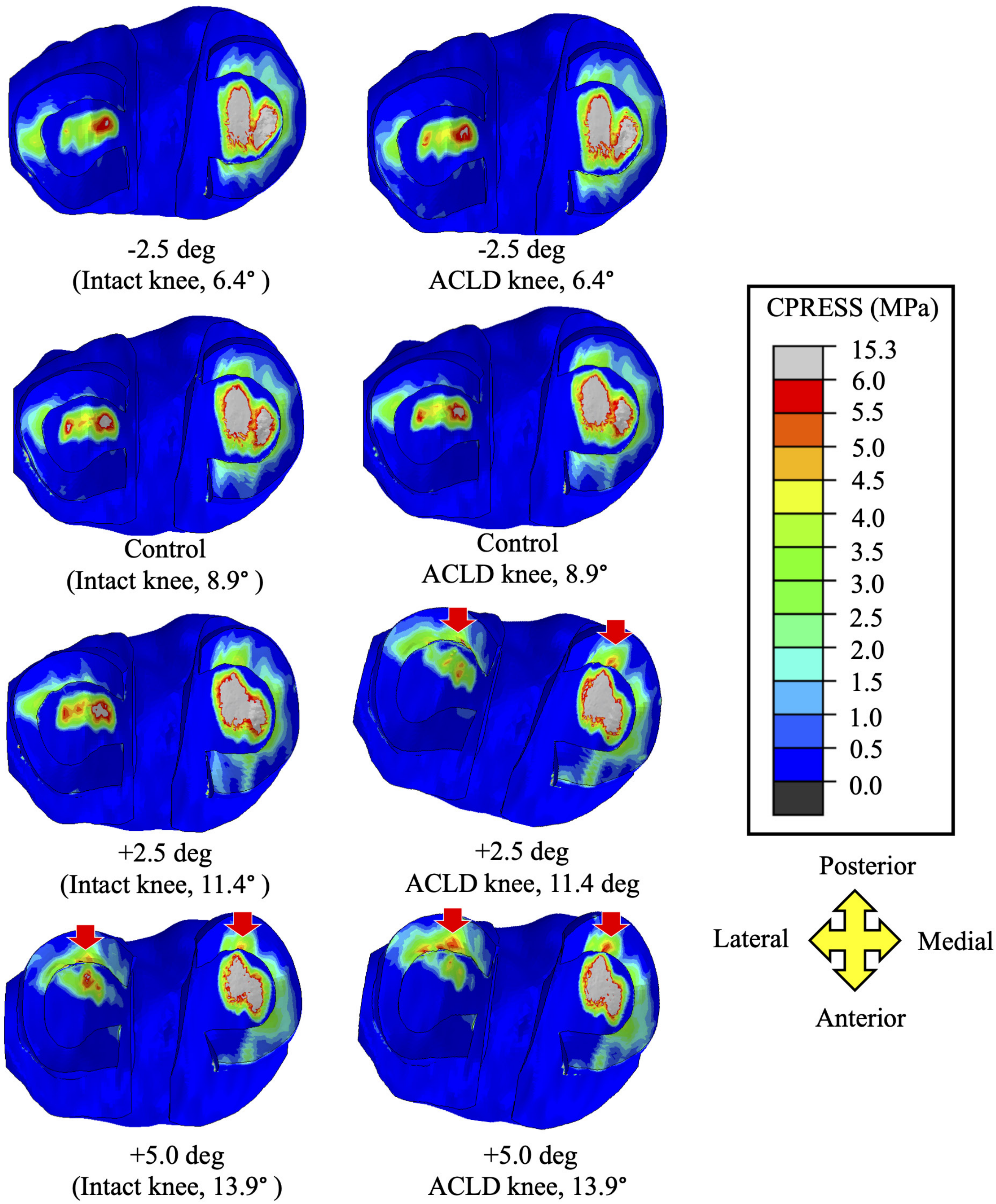

Fig. 5

Comparison of the contact pressure on cartilage and menisci among different simulation conditions at maximum axial loading of the knee (19% of the gait cycle). ACLD, anterior cruciate ligament-deficient.

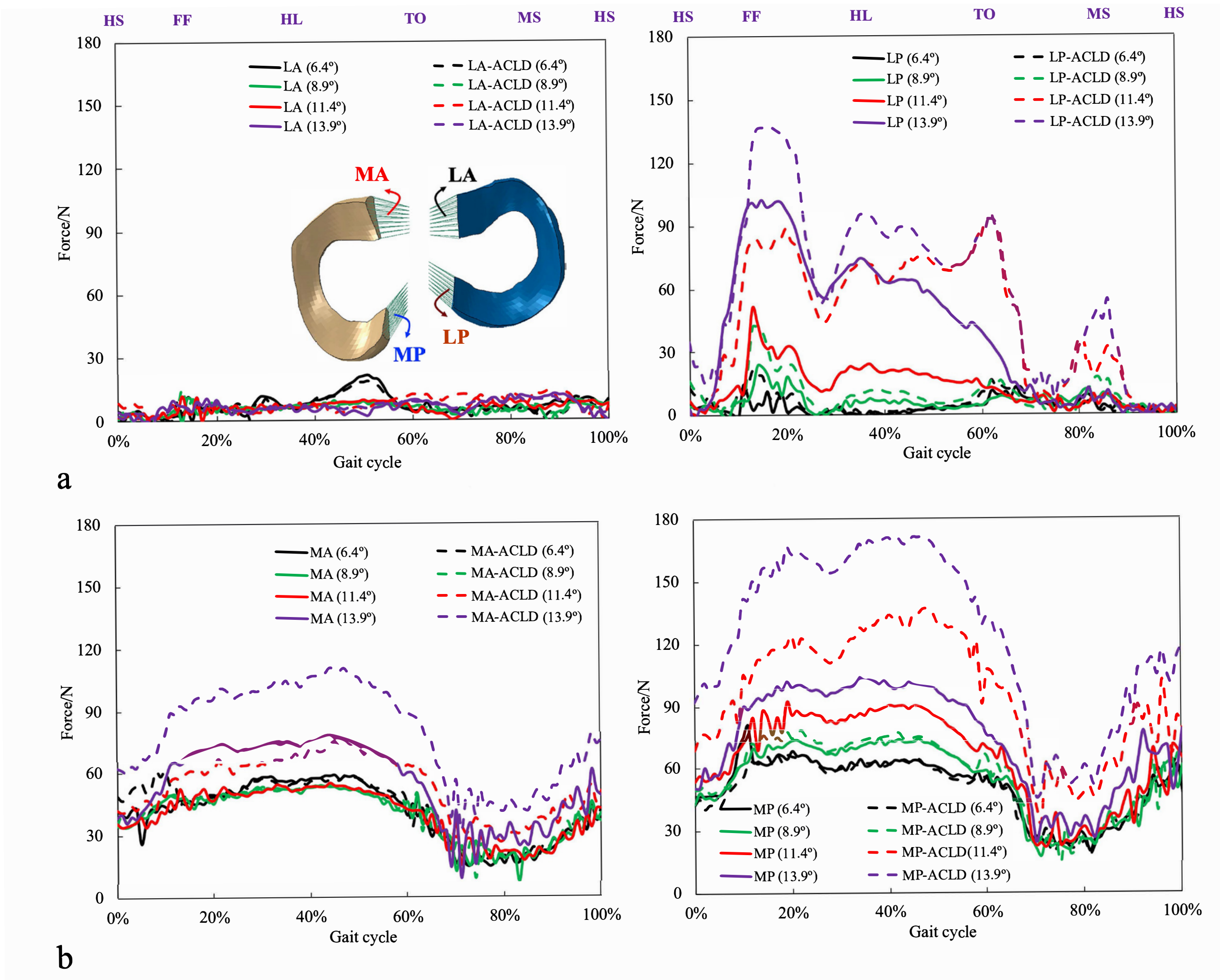

Fig. 6

Predicted tensile force at the horn root of the meniscus. a) Effect of the posterior tibial slope (PTS) angle on the predicted force of the anterior and posterior horns of the lateral meniscus in intact and anterior cruciate ligament-deficient (ACLD) knees. b) Effect of the PTS angle on the predicted force of the anterior and posterior horns of the medial meniscus in intact and ACLD knees. FF, foot flat; HL, heel lift; HS, heel strike; LA, anterior horn of lateral meniscus; LP, posterior horn of lateral meniscus; MA, anterior horn of medial meniscus; MP, posterior horn of medial meniscus; MS, midstance; TO, toe-off.

These findings are consistent with the predicted results at low PTS angles (6.4° and 8.9°), as shown in Figure 4. Furthermore, the co-contraction of muscle around the knee in patients with ACLD may also stabilize the knee.[44,45] In knees with large PTS angles, a much larger tensile force can be found on the ACL during the gait cycle (Figure 3). Thus, the excessive posterior femoral translation would occur due to excessive laxity resulting from ACLD. We observed much smaller differences in AP translation and internal or external (I-E) rotation between intact and ACLD knees at a PTS angle of 13.9°, rather than that of 11.4°. This can be explained by the constraints on the menisci due to the large initial posterior translation (Figure 4).

Contact pressure is the most direct factor to evaluate the risk of tissue damage. The contact areas on the tibial cartilage and menisci are different due to variations in joint kinematics under different conditions of the knee. We observed a level of contact pressure on cartilage that was similar to findings of previous in vitro studies. Bedi et al[46] reported a mean lower maximum contact pressure (7.4 MPa (SD 0.6)) compared to the current study in in vitro experimental tests on a cadaver knee joint with an array of piezoelectric pressure-sensing elements contained within a thin sealed sheet of plastic (4010N; Tekscan, USA) under the guidelines of the International Organization for Standardization (ISO number 14243-1) loading conditions. Degenerative changes in the medial compartment are frequently compensated by the posterior aspect of the meniscus,[17,47] which is consistent with the findings of our study. The medial meniscus has a greater contact pressure than the lateral side, which may suggest a higher risk of medial meniscus tear in the ACLD knee accompanied

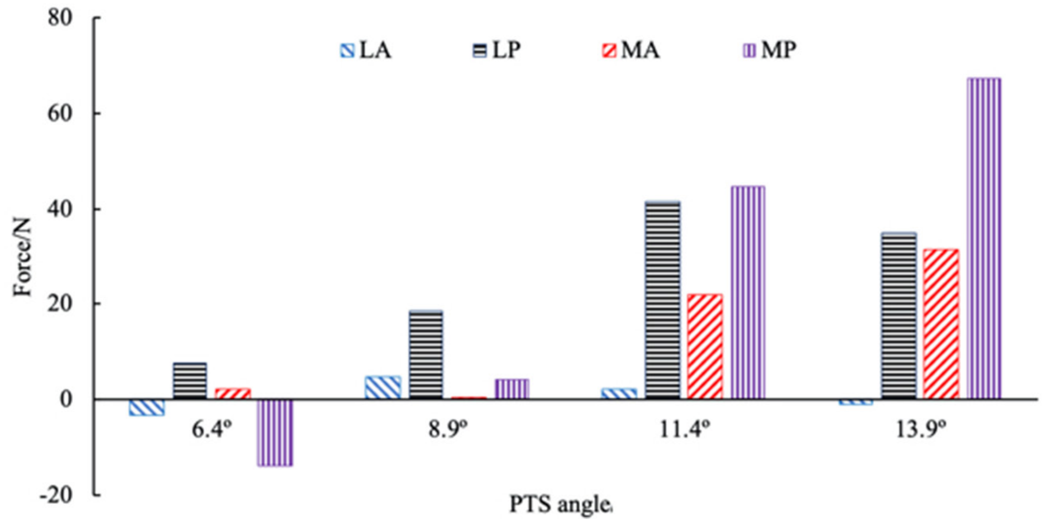

Fig. 7

The change in maximum predicted tensile force in anterior cruciate ligament-deficient (ACLD) knees at the meniscus horn root with the posterior tibial slope (PTS) angle. LA, anterior horn root of the lateral meniscus; LP, posterior horn root of the lateral meniscus; MA, anterior horn root of the medial meniscus; MP, posterior horn root of the medial meniscus.

by a large PTS angle. Mehl et al[48] reported a higher risk of medial meniscus injuries compared to that of the lateral side after reviewing 40 clinical articles related to ACLD knees. The flexibility and mobility of the medial meniscus are much lower than those of the lateral side due to its anatomical characteristics. The medial meniscus tends to restrict the posterior femoral translation to maintain knee stability in ACLD, and this effect is magnified with a larger PTS angle. Furthermore, similar to our findings, Markolf et al[41] highlighted that ACLD knees were particularly susceptible to medial meniscus posterior horn (MP) injury after applying an anterior tibial force, while the anterior tibial force increases significantly with the PTS angle. A much higher tensile force was found in the posterior horn in radial orientation, as shown in Figure 6. This pattern of stress concentration is related to MMPRT, a characteristic of degenerative knee OA. Okazaki et al[49] suggested that the increased posterior slope of the medial plateau is a risk factor for MMPRT.

With steep PTS and ACLD, we observed a higher tensile force on the posterior LP of the lateral meniscus, especially in the inner position, as shown in Figures 5 and 6. This result confirms the clinical finding in which the lateral meniscus showed more flap tears than the medial meniscus. Articular and meniscal pathologies are associated with primary ACL reconstruction;[50] moreover, radial tears were common in the lateral meniscus.[51] More specifically, in the lateral compartment, an increase in slope may have caused rotatory movement under load,[52] and therefore the shear force was concentrated in the inner position of the LP, which is a stabilizer.[53]

This study has some limitations. First, in this study, we did not consider changes in ground reaction forces under different experimental conditions. Second, the gait pattern is affected by ACL injury, which consequently affects the ground reaction force and joint kinematics. These changes should be considered in future studies. Third, this FE-MS framework model system was constructed from only one subject and validated in previous experimental studies.[22–24] Joint kinematics and contact mechanics are subjective and, therefore, can vary between populations. The effect of subjective differences and population-based dynamic performance of the knee joint should be further analyzed. Fourth, we changed the PTS angle by altering the orientation of the tibial plateaus, and the remaining anatomical characteristics were left unchanged. The detailed geometry of the tibial bone, such as shallowness, size, and curvature, may also affect the predicted results.

In conclusion, our study provides fundamental information regarding the effects of the PTS angle on intact and ACLD knees during the gait cycle. We noted a major difference in joint kinematics, contact pressure, and meniscus horn force between the intact and ACLD knees as the PTS angle increased beyond 11.4°, even 2.5° greater than the control. We found that contact pressure increased on the posterior aspect of the medial meniscus and tibial cartilage, which is consistent with the location of degenerative changes following meniscus tear that are frequently found in patients with ACLD. Meniscus injuries are more likely to occur with a larger PTS angle in patients with ACLD during the gait cycle. Our findings provide fundamental information for optimal ligament reconstruction and OA prevention.

References

1. **Louboutin H**, **Debarge R**, **Richou J**, **et al**. Osteoarthritis in patients with anterior cruciate ligament rupture: a review of risk factors. *Knee*. 2009;16(4):239–244.
2. **Hill CL**, **Seo GS**, **Gale D**, **Totterman S**, **Gale ME**, **Felson DT**. Cruciate ligament integrity in osteoarthritis of the knee. *Arthritis Rheum*. 2005;52(3):794–799.
3. **Ren S**, **Yu Y**, **Shi H**, **et al**. Three dimensional knee kinematics and kinetics in ACL-deficient patients with and without medial meniscus posterior horn tear during level walking. *Gait Posture*. 2018;66:26–31.
4. **Defrate LE**, **Papannagari R**, **Gill TJ**, **Moses JM**, **Pathare NP**, **Li G**. The 6 degrees of freedom kinematics of the knee after anterior cruciate ligament deficiency: an in vivo imaging analysis. *Am J Sports Med*. 2006;34(8):1240–1246.
5. **Shabani B**, **Bytyqi D**, **Lustig S**, **Cheze L**, **Bytyqi C**, **Neyret P**. Gait changes of the ACL-deficient knee 3D kinematic assessment. *Knee Surg Sports Traumatol Arthrosc*. 2015;23(11):3259–3265.
6. **Kayani B**, **Konan S**, **Ahmed SS**, **Chang JS**, **Ayuob A**, **Haddad FS**. The effect of anterior cruciate ligament resection on knee biomechanics. *Bone Joint J*. 2020;102-B(4):442–448.
7. **Church S**, **Keating JF**. Reconstruction of the anterior cruciate ligament: timing of surgery and the incidence of meniscal tears and degenerative change. *J Bone Joint Surg Br*. 2005;87-B(12):1639–1642.
8. **Ali AA**, **Harris MD**, **Shalhoub S**, **Maletsky LP**, **Rullkoetter PJ**, **Shelburne KB**. Combined measurement and modeling of specimen-specific knee mechanics for healthy and ACL-deficient conditions. *J Biomech*. 2017;57:117–124.
9. **Chen C-H**, **Li J-S**, **Hosseini A**, **Gadikota HR**, **Gill TJ**, **Li G**. Anteroposterior stability of the knee during the stance phase of gait after anterior cruciate ligament deficiency. *Gait Posture*. 2012;35(3):467–471.
10. **Bernhardson AS**, **Aman ZS**, **Dornan GJ**, **et al**. Tibial slope and its effect on force in anterior cruciate ligament grafts: anterior cruciate ligament force increases linearly as posterior tibial slope increases. *Am J Sports Med*. 2019;47(2):296–302.
11. **Dejour D**, **Pungitore M**, **Valluy J**, **Nover L**, **Saffarini M**, **Demey G**. Preoperative laxity in ACL-deficient knees increases with posterior tibial slope and medial meniscal tears. *Knee Surg Sports Traumatol Arthrosc*. 2019;27(2):564–572.
12. **Arner JW**, **Irvine JN**, **Zheng L**, **et al**. The effects of anterior cruciate ligament deficiency on the meniscus and articular cartilage: a novel dynamic in vitro pilot study. *Orthop J Sports Med*. 2016;4(4):2325967116639895.
13. **Lee J-A**, **Koh Y-G**, **Kim PS**, **Kang KW**, **Kwak YH**, **Kang K-T**. Biomechanical effect of tibial slope on the stability of medial unicompartmental knee arthroplasty in posterior cruciate ligament-deficient knees. *Bone Joint Res*. 2020;9(9):593–600.
14. **Hada M**, **Mizu-Uchi H**, **Okazaki K**, **et al**. Posterior tibial slope and anterior post-cam contact can change knee kinematics in extension in bi-cruciate stabilized total knee arthroplasty. *Bone Joint Res*. 2020;9(11):761–767.
15. **D'Lima DP**, **Huang P**, **Suryanarayan P**, **Rosen A**, **D'Lima DD**. Tibial tray rotation and posterior slope increase risk for outliers in coronal alignment. *Bone Joint J*. 2020;102-B(6_Supple_A):43–48.
16. **Fening SD**, **Kovacic J**, **Kambic H**, **McLean S**, **Scott J**, **Miniaci A**. The effects of modified posterior tibial slope on anterior cruciate ligament strain and knee kinematics: A human cadaveric study. *J Knee Surg*. 2008;21(3):205–211.
17. **Bedi A**, **Chen T**, **Santner TJ**, **et al**. Changes in dynamic medial tibiofemoral contact mechanics and kinematics after injury of the anterior cruciate ligament: A cadaveric model. *Proc Inst Mech Eng H*. 2013;227(9):1027–1037.
18. **Baldwin MA**, **Clary CW**, **Fitzpatrick CK**, **Deacy JS**, **Maletsky LP**, **Rullkoetter PJ**. Dynamic finite element knee simulation for evaluation of knee replacement mechanics. *J Biomech*. 2012;45(3):474–483.
19. **Guess TM**, **Razu S**. Loading of the medial meniscus in the ACL deficient knee: a multibody computational study. *Med Eng Phys*. 2017;41:26–34.
20. **Ali AA**, **Shalhoub SS**, **Cyr AJ**, **et al**. Validation of predicted patellofemoral mechanics in a finite element model of the healthy and cruciate-deficient knee. *J Biomech*. 2016;49(2):302–309.
21. **Fitzpatrick CK**, **Baldwin MA**, **Clary CW**, **Maletsky LP**, **Rullkoetter PJ**. Evaluating knee replacement mechanics during ADL with PID-controlled dynamic finite element analysis. *Comput Methods Biomech Biomed Engin*. 2014;17(4):360–369.
22. **Shu L**, **Yao J**, **Yamamoto K**, **Sato T**, **Sugita N**. In vivo kinematical validated knee model for preclinical testing of total knee replacement. *Comput Biol Med*. 2021;132:104311.
23. **Shu L**, **Yamamoto K**, **Yao J**, **et al**. A subject-specific finite element musculoskeletal framework for mechanics analysis of a total knee replacement. *J Biomech*. 2018;77:146–154.
24. **Shu L**, **Yamamoto K**, **Yoshizaki R**, **Yao J**, **Sato T**, **Sugita N**. Multiscale finite element musculoskeletal model for intact knee dynamics. *Comput Biol Med*. 2022;141:105023.
25. **Delp SL**, **Loan JP**. A graphics-based software system to develop and analyze models of musculoskeletal structures. *Comput Biol Med*. 1995;25(1):21–34.
26. **Erdemir A**. Open knee: open source modeling and simulation in knee biomechanics. *J Knee Surg*. 2016;29(2):107–116.
27. **Blankevoort L**, **Huiskes R**, **de Lange A**. Recruitment of knee joint ligaments. *J Biomech Eng*. 1991;113(1):94–103.
28. **Shahzad M**, **Kamran A**, **Siddiqui MZ**, **Farhan M**. Mechanical characterization and FE modelling of a hyperelastic material. *Mat Res*. 2015;18(5):918–924.
29. **Holzapfel GA**, **Gasser TC**, **Ogden RW**. A new constitutive framework for arterial wall mechanics and a comparative study of material models. *J Elast*. 2000;61(1–3):1–48.
30. **Naghibi Beidokhti H**, **Janssen D**, **van de Groes S**, **Hazrati J**, **Van den Boogaard T**, **Verdonschot N**. The influence of ligament modelling strategies on the predictive capability of finite element models of the human knee joint. *J Biomech*. 2017;65:1–11.
31. **Tissakht M**, **Ahmed AM**. Tensile stress-strain characteristics of the human meniscal material. *J Biomech*. 1995;28(4):411–422.
32. **Kusayama T**, **Harner CD**, **Carlin GJ**, **Xerogeanes JW**, **Smith BA**. Anatomical and biomechanical characteristics of human meniscofemoral ligaments. *Knee Surg Sports Traumatol Arthrosc*. 1994;2(4):234–237.
33. **Gupte CM**, **Smith A**, **Jamieson N**, **Bull AMJ**, **Thomas RD**, **Amis AA**. Meniscofemoral ligaments--structural and material properties. *J Biomech*. 2002;35(12):1623–1629.
34. **Lin LJ**, **Akpinar B**, **Meislin RJ**. Tibial slope and anterior cruciate ligament reconstruction outcomes. *JBJS Rev*. 2020;8(4):e0184.
35. **Todd MS**, **Lalliss S**, **Garcia E**, **DeBerardino TM**, **Cameron KL**. The relationship between posterior tibial slope and anterior cruciate ligament injuries. *Am J Sports Med*. 2010;38(1):63–67.
36. **Ni Q-K**, **Song G-Y**, **Zhang Z-J**, **et al**. Steep posterior tibial slope and excessive anterior tibial translation are predictive risk factors of primary anterior cruciate ligament reconstruction failure: a case-control study with prospectively collected data. *Am J Sports Med*. 2020;48(12):2954–2961.
37. **Komzák M**, **Hart R**, **Okál F**, **Safi A**. AM bundle controls the anterior-posterior and rotational stability to a greater extent than the PL bundle - a cadaver study. *Knee*. 2013;20(6):551–555.
38. **Markolf KL**, **Park S**, **Jackson SR**, **McAllister DR**. Contributions of the posterolateral bundle of the anterior cruciate ligament to anterior-posterior knee laxity and ligament forces. *Arthroscopy*. 2008;24(7):805–809.
39. **Marouane H**, **Shirazi-Adl A**, **Hashemi J**. Quantification of the role of tibial posterior slope in knee joint mechanics and ACL force in simulated gait. *J Biomech*. 2015;48(10):1899–1905.
40. **Samuelsen BT**, **Aman ZS**, **Kennedy MI**, **et al**. Posterior medial meniscus root tears potentiate the effect of increased tibial slope on anterior cruciate ligament graft forces. *Am J Sports Med*. 2020;48(2):334–340.
41. **Markolf KL**, **Jackson SR**, **McAllister DR**. Force measurements in the medial meniscus posterior horn attachment: effects of anterior cruciate ligament removal. *Am J Sports Med*. 2012;40(2):332–338.
42. **Bergmann G**, **Bender A**, **Graichen F**, **et al**. Standardized loads acting in knee implants. *PLoS One*. 2014;9(1):e86035.
43. **Reynolds RJ**, **Walker PS**, **Buza J**. Mechanisms of anterior-posterior stability of the knee joint under load-bearing. *J Biomech*. 2017;57:39–45.
44. **Shanbehzadeh S**, **Mohseni Bandpei MA**, **Ehsani F**. Knee muscle activity during gait in patients with anterior cruciate ligament injury: a systematic review of electromyographic studies. *Knee Surg Sports Traumatol Arthrosc*. 2017;25(5):1432–1442.
45. **Smith CR**, **Brandon SCE**, **Thelen DG**. Can altered neuromuscular coordination restore soft tissue loading patterns in anterior cruciate ligament and menisci deficient knees during walking? *J Biomech*. 2019;82:124–133.
46. **Bedi A**, **Kelly NH**, **Baad M**, **et al**. Dynamic contact mechanics of the medial meniscus as a function of radial tear, repair, and partial meniscectomy. *J Bone Joint Surg Am*. 2010;92-A(6):1398–1408.
47. **Murrell GA**, **Maddali S**, **Horovitz L**, **Oakley SP**, **Warren RF**. The effects of time course after anterior cruciate ligament injury in correlation with meniscal and cartilage loss. *Am J Sports Med*. 2001;29(1):9–14.
48. **Mehl J**, **Otto A**, **Baldino JB**, **et al**. The ACL-deficient knee and the prevalence of meniscus and cartilage lesions: a systematic review and meta-analysis (CRD42017076897). *Arch Orthop Trauma Surg*. 2019;139(6):819–841.

49. **Okazaki Y**, **Furumatsu T**, **Kodama Y**, **et al**. Steep posterior slope and shallow concave shape of the medial tibial plateau are risk factors for medial meniscus posterior root tears. *Knee Surg Sports Traumatol Arthrosc*. 2021;29(1):44–50.
50. **Ghodadra N**, **Mall NA**, **Karas V**, **et al**. Articular and meniscal pathology associated with primary anterior cruciate ligament reconstruction. *J Knee Surg*. 2013;26(3):185–193.
51. **Harper KW**, **Helms CA**, **Lambert HS**, **Higgins LD**. Radial meniscal tears: significance, incidence, and MR appearance. *AJR Am J Roentgenol*. 2005;185(6):1429–1434.
52. **Simon RA**, **Everhart JS**, **Nagaraja HN**, **Chaudhari AM**. A case-control study of anterior cruciate ligament volume, tibial plateau slopes and intercondylar notch dimensions in ACL-injured knees. *J Biomech*. 2010;43(9):1702–1707.
53. **Musahl V**, **Citak M**, **O'Loughlin PF**, **Choi D**, **Bedi A**, **Pearle AD**. The effect of medial versus lateral meniscectomy on the stability of the anterior cruciate ligament-deficient knee. *Am J Sports Med*. 2010;38(8):1591–1597.

Author information:
- L. Shu, PhD, Professor, Research into Artifacts, Center for Engineering, School of Engineering, The University of Tokyo, Tokyo, Japan; Department of Mechanical Engineering, School of Engineering, The University of Tokyo, Tokyo, Japan; Department of Mechanical Engineering, Dalian University of Technology, Dalian, China.
- N. Abe, MD, PhD, Professor, Department of Orthopaedic Surgery and Sport Medicine, General Medical Center, Kawasaki Medical School, Okayama, Japan.
- S. Li, PhD, Postdoctoral researcher
- N. Sugita, PhD, Professor

  Research into Artifacts, Center for Engineering, School of Engineering, The University of Tokyo, Tokyo, Japan; Department of Mechanical Engineering, School of Engineering, The University of Tokyo, Tokyo, Japan.

Author contributions:
- L. Shu: Data curation, Formal Analysis, Funding acquisition, Investigation, Methodology, Resources, Software, Validation, Visualization, Writing – original draft.
- N. Abe: Conceptualization, Methodology, Project administration, Supervision, Writing – review & editing.
- S. Li: Data curation, Formal Analysis, Investigation, Resources, Software, Validation, Visualization.
- N. Sugita: Funding acquisition, Methodology, Project administration, Supervision.

Funding statement:
- The authors disclose receipt of the following financial or material support for the research, authorship, and/or publication of this article: funding support from JSPS KAKENHI (Grant Number 20K20162).

ICMJE COI statement:
- The authors have no conflict of interest to report.

Acknowledgements:
- Ethics approval for the experimental procedures was granted by the Human Research Committee at the University of Tokyo (approval number: KE16-51), Japan.

Open access funding
- The authors report that the open access funding for their manuscript was self-funded.